



Improving Spectrum Efficiency in 5G Networks via Collaborative Spectrum Sharing for MIMO-NOMA Enhancement

Bharathi C. ¹, Manjunatha Reddy H. S. ^{2*}

¹ Associate Professor, Dept. of ECE, Global Academy of Technology, Bengaluru-98, India

² Professor and Head, Dept. of ECE, Global Academy of Technology, Bengaluru-98, India

*Corresponding Author: manjunathareddyhs@gmail.com

Citation: B. C and M. R. H. S, "Improving Spectrum Efficiency in 5G Networks via Collaborative Spectrum Sharing for MIMO-NOMA Enhancement," *International Journal of Communication Networks and Information Security (IJCNIS)*, vol. 16, no. 2, pp. 1-15, Jun. 2024.

ARTICLE INFO

Received: 15 November 2023
Accepted: 29 February 2024

ABSTRACT

This research utilises two innovative ways to improve the spectrum efficiency of the 5G Downlink Non-Orthogonal Multiple Access (NOMA) power domain. Enhancements are achieved by a Cooperative Cognitive Radio Network (CCRN). Single-Input Single-Output (SISO), Multiple-Input Multiple-Output (MIMO), and Massive Multiple-Input Multiple-Output (M-MIMO) configurations are evaluated within a single cell of a communication network. NOMA users initially compete for CCRN common control channels. NOMA customers are given high-priority dedicated control channels during the second approach. The proposed approaches are assessed using MATLAB for three parameters: distance, power localization coefficient, and transmission power scenarios. Simulation involves four users utilizing 80 MHz bandwidths and Quadrature Phase-Shift Keying (QPSK) modulation. We examine successive interference cancellation and channel instability assuming that Rayleigh signal fades with frequency. User 4 attained the best Spectral efficiency compared to the other four users, achieving 3.9 bps/Hz/cell for SISO Downlink NOMA, 5.1 for CCRN using common channels, and 7.2 for dedicated control channels. The findings were achieved at a transmit power of 40 dBm. User 4, the top performer, attained a spectral efficiency of 51% utilising a 64 x 64 MIMO Downlink NOMA system. At 40 dB transmit power, common control channels and dedicated control channels improved spectral efficiency performance by 64% and 65% respectively compared to SISO Downlink NOMA. Moreover, 128 × 128 M-MIMO Downlink NOMA improved spectral efficiency performance by 79% for the highest-ranked U4 user. When compared to SISO Downlink NOMA at 40 dB transmit power, The CCRN combining common control channels and dedicated control channels improved spectral efficiency performance by 85% and 86%, respectively. According to the study, the second suggested choice, dedicated control channels with Cooperative Cognitive Radio NOMA (CCR-NOMA), provides clients with the maximum spectrum efficiency. MIMO and M-MIMO enhance spectrum efficiency.

Keywords: Massive Multiple-Input Multiple-Output, Cooperative cognitive radio networks, Downlink, Dedicated control channels, Quadrature Phase-shift Keying.

INTRODUCTION

NOMA is widely acknowledged as a crucial technology that paves the way for the future of wireless communication networks. It boosts the spectrum efficiency of the system and ensures a more equitable distribution of network resources among users. Superposition coding lies at the heart of NOMA, which relies on base stations to differentiate between signals from various users, and mobile receivers employ a process known as successive interference cancellation to clear up signal overlap[1].

NOMA's essence lies in its ability to cater to multiple users simultaneously through time or data rate

differentiation. The quantity of users it can accommodate is directly influenced by the availability of orthogonal resources[2]. NOMA operates in two main domains: the power domain, where users transmit at varying power levels over the same spectral or temporal resource, and the code domain, where a unique code book is designed for each user's data. This approach significantly boosts the capacity and efficiency of future wireless systems to meet the growing data demand. The advancement of mobile networks will involve a notable improvement in resource utilization efficiency, in part by enabling more users to dynamically share the spectrum[3].

However, the finite nature of the available frequency spectrum poses a challenge, necessitating innovative strategies to cater to growing traffic needs and mitigate potential spectrum scarcity. Cognitive radio technology emerges as a solution, facilitating spectrum sharing between primary and secondary users under conditions that minimize interference[4].

A pivotal study introduced essential processes in cognitive radio, discussing two key spectrum-sharing methods that optimize radio frequency utilization while preventing interference between traditional and cognitive radio networks[5]. Despite advancements in MIMO-NOMA for cooperative spectrum sensing in cognitive radio networks, there remain gaps in understanding access methods and user capacity in large-scale networks[6], [7], [8], [9].

This research aims to enhance network efficiency and throughput, especially when primary users face channel issues, by activating cooperative cognitive radio within the same network or cell in 5G through specific channels. This initiative is part of broader efforts to integrate downlink power domain NOMA with cooperative cognitive radio, employing both SISO and various MIMO configurations to surpass the spectrum efficiency of traditional models[10], [11], [12], [13]. Furthermore, this work proposes a method to quantify the effectiveness of these integration, taking into account different design parameters to boost performance. The basic block diagram for the MIMO-NOMA signal detection is presented in Figure 1.

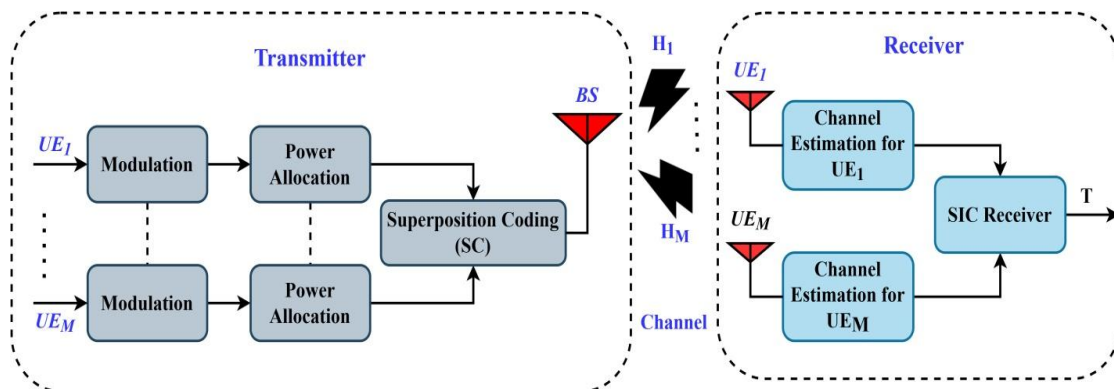


Figure 1. General Block Diagram of MIMO NOMA Signal Detection

Given the limited frequency spectrum available for wireless applications, exacerbated by scarcity and spectral constraints, there is an increasing need for innovative solutions to meet the growing demand for communication services. Cognitive Radio (CR) has emerged as a key strategy to address the above challenges like spectrum scarcity, enabling secondary users to utilize the spectrum originally allocated to primary users under conditions that minimize interference[14].

This study introduces a critical process within cognitive radio, showcasing two effective strategies for sharing the spectrum that enhance radio frequency utilization without causing disruption. It carried out the previous research work that categorizes spectrum access strategies and explores different approaches to spectrum usage. Implementing cognitive radio networks equipped with advanced NOMA technology and MIMO capabilities, this approach aims to boost network capacity even in challenging conditions like Additive white Gaussian noise and Rayleigh fading. Yet, recent literature highlights a gap in understanding cognitive radio network access methods, a significant underestimation of user representation, and a lack of attention to power-location dynamics.

The main contribution of this research is the activation of cooperative cognitive radio within a unified 5G network and cell to address issues of channel instability or unavailability for primary users. This activation, whether through a common or a dedicated control channel, is designed to significantly enhance network throughput and efficiency. A notable aspect of this study is the dual-method integration of downlink power domain NOMA with cooperative cognitive radio in the 5G framework, utilizing both SISO and MIMO configurations, including massive MIMO setups. This integration demonstrates a marked improvement in spectrum efficiency over traditional SISO downlink NOMA models. Additionally, the research establishes a framework for quantitatively measuring performance enhancements across a range of design parameters.

In this research work, there are three main contributions to wireless communication and network optimization are presented.

Firstly, in this research work we have proposed two novel techniques that were used to improvise the spectral efficiency of downlink NOMA power domain in conjunction with a CCRN within a 5G network. In the first approach, whenever the primary users experience the unavailability of the channel, then it will activate the cooperative cognitive radio within the same network and within the single cell in 5G by a common control channel or through a dedicated channel.

In the 5G network, we have implemented downlink NOMA power domain with cooperative cognitive radio in two different ways with SISO & MIMO. From the above techniques implemented with cooperative cognitive radio, we can observe the improvement in spectral efficiency to that of SISO.

Lastly, the evaluation of these proposed approaches in this research work is carried out with the help of MATLAB software across various parameters taking into consideration varying distances, varying power coefficients, and transmitting power levels as stated. This extensive evaluation provides detailed insights into the performance of a system across diverse scenarios, thus ensuring that the proposed approaches are practically feasible across different conditions.

The structure of this article is as follows: Section 2 presents a literature survey of research efforts that were previous to and interrelated with this. Section 3 develops the mathematical model for the proposed system. Based on the proposed system, their simulation with corresponding parameters is developed using MATLAB is discussed in Section 4. The results are made in Section 5 of the paper and the paper concludes itself in Section 6 providing an overview of possible future work.

LITERATURE REVIEW

This section outlines the benefits and drawbacks of some of the various existing power distribution strategies for MIMO-NOMA networks. Dai L et al. [1] developed and implemented an energy allocation system for electricity to improve energy efficiency. The study in [14] delves into the analysis of the CR-NOMA system, with a special focus on both outage probability and throughput. This study is concerned with developing closed-form expressions for outage probability tailored for assessing the performance of secondary network users in the environment of primary network interference. Numerically, the results underline the significance of proper power configuration and energy efficiency parameters to ensure equitable performance in the system for all users. Besides assessing the CR-NOMA system, the author investigates MIMO-CR-NOMA Internet of Things (IoTs) frameworks, taking into account the spectral structure.

In addition, this study computes the throughput per user as well as the total throughput, which enables it to provide a thorough perspective of the system performance. It is clear that the author has conducted a thorough investigation into the complexities of the system in order to develop communication solutions that are simple to use. CR orthogonal multiple access (CR-OMA), CR-NOMA, CR-MIMO, and MIMO-CR-NOMA are some of the scenarios that are discussed in the following paper [15], in which the authors explain how to compute the frame rate for these scenarios. Real-world problems in communication systems can be analyzed in a more thorough manner if certain factors, such as non-linear channels and sub-optimal channel conditions, are taken into consideration.

After that, the author is going to concentrate on a problem that occurs in a multi-carrier NOMA system with the intention of enhancing the system's efficiency. Integrating a Cognitive Radio Network base into the multi-carrier NOMA network is an efficient method that may be utilize to improve the system's overall throughput while simultaneously minimizing the impact on the throughput of primary users. The author's dedication to enhancing system performance by considering different network components is demonstrated in this innovative technique, as described in [16]. In an alternative realm of the investigation, [17] provides asymptotic formulas for a NOMA-based overlay cognitive radio network specifically designed for Industry 5.0. The analytical formulas for outage probability and ergodic rate offer valuable insights into the performance of both main and secondary users. The author examines the impact of phase, capacitance, and power distribution on system performance by using simulation. This approach provides a comprehensive understanding of several aspects linked to communication systems.

Continuing the exploration of multi-carrier NOMA systems, [18] introduces a low-complexity resource allocation approach aimed at meeting user fairness requirements. Its balance in energy efficiency along with spectrum efficiency outperforms recent methods while keeping complexity low. This validates the higher energy and spectrum efficiency of the proposed NOMA system in real-world implementations. An interesting twist in the

study of NOMA cognitive systems is taken in [19], where blocking probability is considered jointly with imperfect successive cancellation interference. The use of closed models to assess outage probabilities for primary and secondary users, supplemented by simulations, guarantees the reliability and accuracy of the performance study results regarding the system's behavior.

Regarding smart surfaces, [20] investigates the use of active refracting and passive reflective Re-configurable Intelligent Surfaces (RIS) to improve secrecy performance in an IoT network. The power allocation, phase shifts and transmit beam-forming are coordinated to optimize the weighted sum secrecy rate. The simulated findings offer empirical proof of the efficiency of the design, hence emphasizing the significance of intelligent surfaces in improving communication security. [21] offers a collaborative optimization strategy for a NOMA-based Satellite–Terrestrial Integrated Network (STIN), sharing the millimeter-wave spectrum between a satellite multicast communication network and a cellular network utilizing NOMA technology. The simulation results have proved the superiority of the suggested strategy, under the assumption of specified antenna designs for the satellite and base station.

In accordance with the discussion in reference[22], the research goes further into the subject of beam-forming in multi-beam satellite systems that are both safe and efficient in terms of energy consumption. The technique has been developed with the explicit intention of maximizing the secrecy energy efficiency while following to the budget constraints of total transmit power. The results of the simulation make it abundantly evident that the suggested method outperforms all benchmark schemes, highlighting the simplicity of the proposed method in comparison to methods that are already in existence and are more complex. A study highlights the effectiveness of active refracting RIS-based transmitters and passive reflective RIS in terms of maximizing the weighted sum secrecy rate. This is done in order to ensure that the information is kept confidential. Additionally, the study reveals how intelligent surfaces can improve the safety of communication. In order to provide a concise summary of the comprehensive research, [23] suggests a technique known as Partial Collaborative Zero-impact (PCZF) for large-scale, cell-free uplink MIMO systems. To reduce the amount of interference that is brought about by zero-effect decoding, the technology enhances performance by making it easier for access points to work together by exchanging Channel State Information. The findings from the numerical analysis provide support for the theoretical study and indicate the effectiveness of the energy control measures that were recommended.

Essentially, all the papers considered in this work reflect comprehensive and complex research on different aspects of communication systems, from CR-NOMA systems to intelligent surfaces and satellite communication networks. Through meticulous attention to detail, innovative problem-solving, and empirical validation through simulations, the knowledge in this field has advanced, opening ways for practical implementations and gearing up further research.

METHODOLOGY

This article will discuss some of the fundamentals of downlink and uplink NOMA, along with the assumption that 'm' users in a cluster have different channel gains in this section. Multiple signals are superimposed using power domain multiplexing and then decoded using a successive interference cancellation process at the receiver side.

Single Input Single Output Downlink NOMA(SISO NOMA)

Specifically, the analysis was carried out for three different scenarios, each of which featured three different models, as will be discussed in detail in the following section. Figure 2 illustrates the SISO Downlink NOMA system, which does not have any multiple antenna elements. This system is presented for consideration. The NOMA system is able to function both with and without the incorporation of CCRN for the purpose of providing free and dedicated channels within a single network and cell. U_1 , U_2 , U_3 , and U_4 are the four NOMA users that are located at different distances from the base station, which are represented by the symbols d_1 , d_2 , d_3 , and d_4 , respectively. It is important to note that U_1 , which is located further away from the base station, is anticipated to receive a weaker signal in comparison to U_4 , which is located closest to the base station. The Rayleigh fading coefficients that correspond to users are represented by the symbols h_1 , h_2 , h_3 , and h_4 , while the current power coefficients are designated by the symbols α_1 , α_2 , α_3 , and α_4 , respectively.

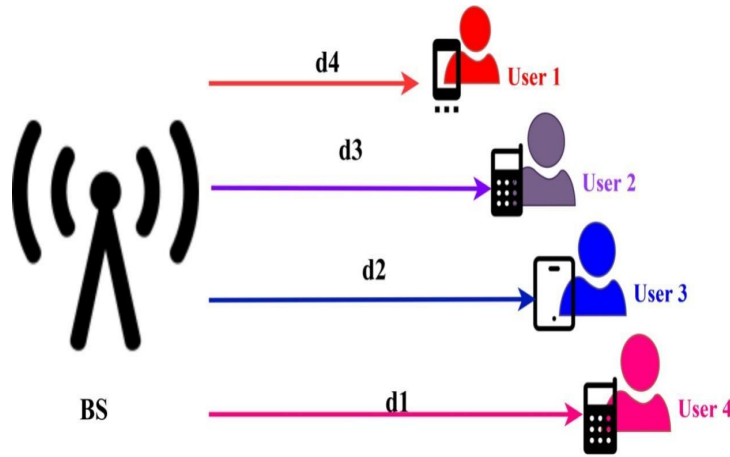


Figure 2. Wireless Network with Four Users (Downplay-NOMA Power Domain)

In accordance with the rules of the NOMA power domain, the user who has a stronger signal (which is located closer to the base station) is given less power, while the user who has a weaker signal (which is located further away from the base station) is given more power. Because of this allocation, the adjusted power coefficients, which are denoted as x_1 , x_2 , x_3 , and x_4 , are reflected. There are a number of different dynamic power coefficient strategies that can be utilized to improve efficiency. The QPSK signals that are transmitted to the base stations are controlled by these adjusted power coefficients, which are denoted by x_1 , x_2 , x_3 , and x_4 . The mathematical expression for the encoded overlay signal that is received by the base station is $x = \sqrt{P}(\sqrt{\alpha_1}x_1 + \sqrt{\alpha_2}x_2 + \sqrt{\alpha_3}x_3 + \sqrt{\alpha_4}x_4)$. The signal that is received by the i th user is represented by the equation $y_i = h_i x + n_i$, where n_i is the additive white Gaussian noise that the i th user (U_i) encounters. For the purpose of decoding y_1 , the strongest signal, which interacts directly with the other three signals, is implemented. The maximums that are attainable are presented in equation 1, and in the event that certain adjustments are made, they might be written as equation 2.

$$R_1 = \log_2 \left(1 + \frac{\alpha_1 P |h_1|^2}{\alpha_2 P |h_1|^2 + \alpha_3 P |h_1|^2 + \alpha_4 P |h_1|^2 + \sigma^2} \right) \quad (1)$$

$$R_1 = \log_2 \left(1 + \frac{\alpha_1 P |h_1|^2}{(\alpha_2 + \alpha_3 + \alpha_4) P |h_1|^2 + \sigma^2} \right) \quad (2)$$

Equation (2) reveals that the power coefficient of the intended user (α_1) should satisfy the condition $\alpha_1 > \alpha_2 + \alpha_3 + \alpha_4$, as the denominator is the sum of power coefficients from the other three users ($\alpha_2 + \alpha_3 + \alpha_4$). The power of the first user (U_1) is dominated by the transmitted signal x and the received signal y_1 . Moving to the equation for the second user (U_2) rate, U_1 's data is considered interference and eliminated due to $\alpha_2 < \alpha_1$, and $\alpha_2 > \alpha_3 > \alpha_4$ using successive interference cancellation. After U_1 's data is deleted, the achieved rate is U_2 . The third user's rate, y_3 , is influenced by U_1 , U_2 , U_3 , and U_4 ($\alpha_3 < \alpha_1$, $\alpha_3 < \alpha_2$), with overlapping terms in the denominator requiring three SIC functions. Finally, the fourth user's rate, y_4 , affected by U_1 , U_2 , U_3 , and U_4 ($\alpha_3 < \alpha_1$, $\alpha_3 < \alpha_2$, $\alpha_3 < \alpha_4$), necessitates two SIC functions for removed data. The attainable rate is expressed in equation 6, with the elimination of α_1 followed by the removal of the α_3 term.

$$R_2 = \log_2 \left(1 + \frac{\alpha_2 P |h_2|^2}{\alpha_3 P |h_2|^2 + \alpha_4 P |h_2|^2 + \sigma^2} \right) \quad (3)$$

$$R_3 = \log_2 \left(1 + \frac{\alpha_3 P |h_3|^2}{\alpha_4 P |h_3|^2 + \sigma^2} \right) \quad (4)$$

$$R_4 = \log_2 \left(1 + \frac{\alpha_4 P |h_4|^2}{\sigma^2} \right) \quad (5)$$

CCRN-based Free Channels

Consider a wireless network comprising four NOMA users (U_1 , U_2 , U_3 , and U_4), with respective power coefficients ($\alpha_3 < \alpha_1$, $\alpha_3 < \alpha_2$), and a CCR network depicted in Figure 3. Distances from the base station for each user are denoted as d_1 , d_2 , d_3 , and d_4 . In terms of the bus station usage, U_1 is identified as the weaker and farther

user, while U4 is considered the stronger and nearer user. Rayleigh fading values are represented using the formula $|h_1|^2|h_2|^2|h_3|^2|h_4|^2$.

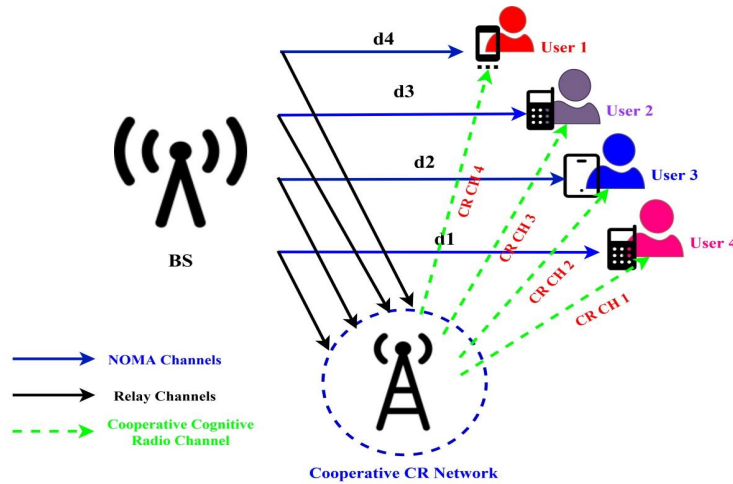


Figure 3. Downplay-NOMA Power Domain with the CCR Network

The investigation into the CCR spectrum involves assessing the channel status and its potential for communication. In the case of an unstable channel status and weak communication, two options are considered: the availability or unavailability of the CCR channel. If CCR channels are available then NOMA can use those channels and CR must utilize the entire period of spectrum window for packet transmission (s) within a period designated as T_s . This period satisfies the relation [24]:

$$T_{\text{window}} \geq T_{\text{sense}} + T_{\text{CR}} - \text{Transmission} + T_{\text{ramp}} - \text{up} + T_{\text{ramp}} - \text{down} \tag{6}$$

Within this context, T_{sense} is a representation of the minimal sensing period that is necessary for the acquisition of key communication characteristics and the occurrence of CR transmission chances. The term "TCR Transmission" refers to the period during which CR packets are transmitted, and "Tramp up/down" refers to the period during which the transmission may ramp up or down. CR transmission opportunity window with fixed beacon signal separation is depicted in Figure 4, which can be found for reference [25].

$$PD = \frac{\text{Number of acquisitions}}{\text{Total number of Opportunities}} = \frac{\text{Over}_{\text{Num}}}{\text{NOP}} \tag{7}$$

In a single primary system, link-level targets are used for spectrum sensing to generate two possible hypotheses: H_0 , which states that there is no primary user signal, and H_1 , which states that a primary user signal is there. In making a sensing choice, factors such as the primary user's broadcast signal $s[n]$, the received complex signal $y[n]$, additive white Gaussian noise $w[n]$, ideal channel complex gain 'h', and observation interval 'N' are taking into account. There are two main types of spectrum sensing techniques: those that rely on energy and those that rely on features [26].

$$y[n] = \begin{cases} w[n]h s[n] & H_0 \\ w[n] & H_1 \end{cases} \quad n = 1 \dots N \tag{8}$$

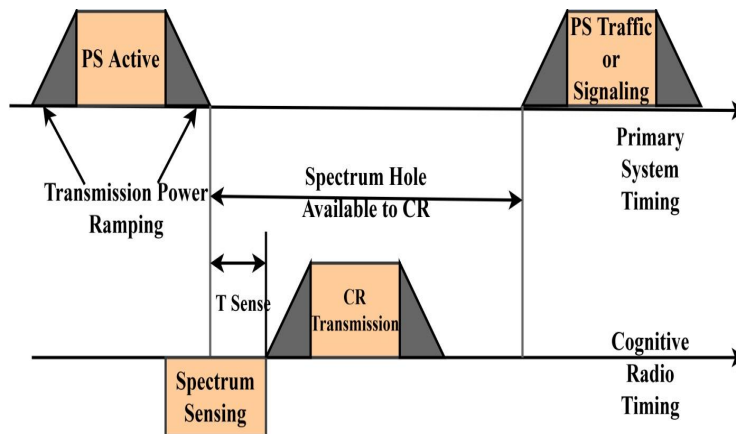


Figure 4. The Opportunity Window for CR Transmission

The process of energy detection is one of these methods, and it entails integrating and quadrupling the signal

that is received across the observation interval. Following this, a comparison is made between the output of the integrator and a threshold in order to arrive at a binary judgement regarding the presence of the principal user.

$$\begin{cases} H_0, & \text{if } \sum_{n=1}^N |y[n]|^2 \leq \lambda \\ H_1, & \text{Otherwise} \end{cases} \quad (9)$$

where λ is the threshold that is affected by the receiver noise.

$$PF = P\left(\frac{H_1}{H_0}\right) = P\left(\frac{P_u}{H_0}\right) = P\left(\frac{Y_n}{H_0}\right) = 1 - P_{H_0}(T_h) \quad (10)$$

ideal channel, and N represents the observation interval. If the channel is not per

In the domain of signal processing, the detection probability is symbolized as PD, the threshold is marked as T_h , and the signal-to-noise ratio is represented by L . Furthermore, the likelihood of failing to detect an event is represented as P_M , whereas the probability of incorrectly identifying a non-event as an event is designated as PFA [27]. The likelihood of inaccuracy in this situation is contingent upon these criteria.

$$PD = \frac{\text{Number of acquisitions}}{\text{Total number of opportunities}} = \frac{\text{Over_Num}}{\text{NOP}} \quad (11)$$

$$PD = 1 - P_M = 1 - P\left(\frac{H_0}{H_1}\right) \quad (12)$$

$$PD = \left[e^{-\frac{T_h}{2}} * \frac{1}{n!} \left(\frac{T_h}{2}\right)^n \right] + \left[e^{-\frac{T_h}{2}} * \left(\frac{1+L}{L}\right) \right] - \left[e^{-\frac{T_h}{2}} * \frac{1}{n!} * \frac{T_h * L}{2(1+L)} \right] \quad (13)$$

$$P_m = 1 - PD \quad (14)$$

When the detection probability is denoted by PD, the threshold is denoted by T_h , and the signal-to-noise ratio is denoted by L , the probability of missed detection is denoted by P_m , and the probability of false alarm is denoted by PFA [28].

The probability of error,

$$P_e = P_p * P_{(H_0)} + P_M r_i P_{(H_1)} \quad (15)$$

CCR-based Dedicated Channel

When the primary communication system is active or the channel state is unstable, the CCR is examined for its potential in communication. This is especially true in situations where the channel state is unstable. In these kinds of circumstances, the CCR channel is seen as being available (high priority), which enables NOMA users to take advantage of it, as shown in Figure 2.

MIMO Downlink PD NOMA

For the case of 64x64 MIMO Downlink NOMA power domain, 64x64 MIMO Downlink NOMA power domain with CCRN common control channel, and 64x64 MIMO Downlink NOMA power domain with CCRN dedicated channel, assuming N users ($U_1, U_2, U_3, \dots, U_N$) in a single cell in a 5G network with power coefficients ($\alpha_2 < \alpha_1, \alpha_3 < \alpha_2, \alpha_4 < \alpha_2$), the probability of error is expressed using NOMA power allocation coefficients a [29]. The transmit antennas simultaneously broadcast x , and the received signal at the base station is analyzed for each user.

$$x = \sqrt{p} (\sqrt{\alpha_1}x_1 + \sqrt{\alpha_2}x_2 + \sqrt{\alpha_3}x_3 + \sqrt{\alpha_4}x_4) \quad (16)$$

Equation 17 is used to determine the Rayleigh fading channel for each individual user. In this formula, the user number is denoted by the letter i ($i = 1, 2, 3, 4$), the total number of channels currently available is denoted by the letter k ($k = 64$), and the signal is received by the base station. Within the scope of this analysis, the channel state and the communication possibilities it offers are taken into consideration, and the CCR spectrum is also introduced. When the channel state and communication are both unstable, the CCR channel's state presents two possibilities: a common control channel or a dedicated channel [30]. Both of these options are available to the user.

$$y_N = xh_{N1} + xh_{N2} + \dots xh_{NN} \quad (17)$$

$$h_{ik} = \sum_{i=1}^k h_{ik} \quad (18)$$

$$y = \sqrt{P_{x1}}h_{1N} + \sqrt{P_{x2}}h_{2N} + \sqrt{P_{x3}}h_{3N} + \sqrt{P_{x4}}h_{4N} \quad (19)$$

M-MIMO Downlink NOMA Power Domain

In the context of 128x128 M-MIMO Downlink NOMA power domain, this section considers three scenarios: 128x128 M-MIMO Downlink NOMA power domain with a CCRN common control channel, and 128x128 M-MIMO Downlink NOMA power domain with a CCRN dedicated Channel. The wireless network in question involves four users, referred to as U1, U2, U3, and UN4. These users are positioned at different distances from each other, and their power coefficients satisfy the conditions $\alpha_2 < \alpha_1$, $\alpha_3 < \alpha_2$, and $\alpha_4 < \alpha_3$. All users are employing the 128x128 M-MIMO Downlink NOMA power domain system under identical conditions as previously specified.

The evaluation approach utilises a standardised methodology to appraise the present precision of the channel and its appropriateness as a means of communication. NOMA users can employ the CR channel once it is operational. NOMA users can access the CCR frequency with a high level of priority, although the core notion remains unaltered[31]. The Rayleigh fading channel for each user can be computed using the identical methodology for analysis.

We employ a standardized method to evaluate the present precision and feasibility of the channel as a means of communication. Within the framework of NOMA, users can choose to employ the CR channel if it is considered to be functional. The core principle remains unaltered, enabling NOMA users to effortlessly access the CCR frequency.

$$h_{jM} = \sum_{j=1}^M h_{jM} \quad (20)$$

where $j = 1, 2, 3, 4$ is the number of users; $M = 128$ is the total number of available channels.

RESULTS AND DISCUSSIONS

To demonstrate the working of the model we have used MATLAB software tool to develop the Downlink NOMA power domain in 5G networks, in which we used both MIMO and M-MIMO architectures. In addition to the above architecture settings, the system model for these technologies was put into action. The set up for the simulation is presented in Table 1. The simulations were carried out and evaluated by considering 3 scenarios, the figures show the calculation of spectral efficiency with respect to power transmission for Downlink NOMA power domain and CCRN with SISO. During this evaluation process, we have considered 64×64 MIMO and 128×128 M-MIMO configurations within the same network and single cell.

Table 1. Simulation Parameters for Uplink & Downlink NOMA

Simulation Parameters				
Sr.No	Parameters	Values		
1	No of Users	4 Users		
2	Transmit Power	0 to 30 dBm		
3	Bandwidth	BW - 80Mhz		
4	Distances	User 1		900m
		User 2		700m
		User 3		400m
		User 4		200m
5	Power Coefficients	User 1		0.75
		User 2		0.19
		User 3		0.054
		User 4		0.013
6	Path Loss exponent	4		
7	SISO	1X1		

Sr.No	Parameters	Values
8	MIMO	64 X 64
9	M-MIMO	128X128
10	Modulation	QPSK

SISO Downlink NOMA Power Domain

Figure 5 depicts the correlation between the Spectral efficiency & Transmit power for the case of SISO Downlink NOMA having varied power coefficients for the four users namely U1, U2, U3 & U4 respectively. All the 4 users (U1 to U4) are located at the distance of 900m, 700m, 400m & 200m respectively from the Base station having the power coefficients of 0.75, 0.188, 0.047, and 0.011. From the graph, one can measure that there is a positive correlation as the transmit power increases there is an increase in the spectral efficiency. The performance of the highest spectral efficiency about 3.9 bps obtained from the user 4 which was physically near the base station and had a power level of 30 dbm. Consequently, the spectral efficiency gradually reduced as we moved from user 3 to user 1 respectively.

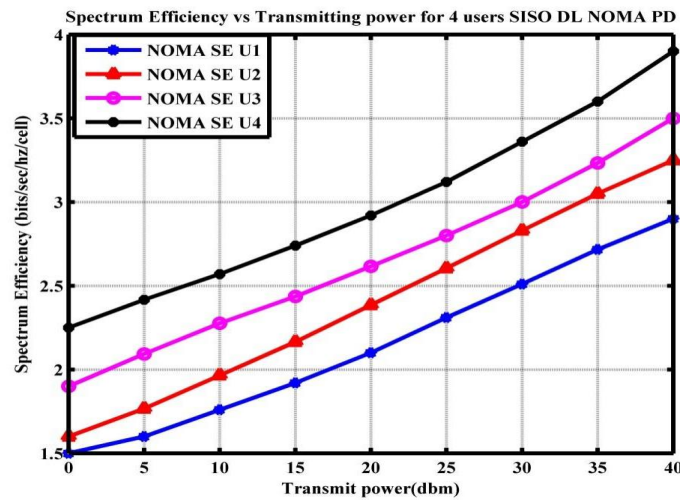


Figure 5. Spectral efficiency vs. Transmitting power for SISO

The link between spectral efficiency and transmitting power is depicted in Figure 6. This relationship is shown for four users, each of whom is positioned at a different distance from the transmitter and is equipped with a distinct power location coefficient. The integration of SISO Downlink NOMA power domain with the CCRN is the subject of this discussion. More specifically, the use of the common control channels free channel in the first model is being discussed. Specifically, the peak spectral efficiency achievement is observed for user U4 when the transmit power is adjusted to 30 dBm. This is a noteworthy achievement because it is recorded at 5.09 bps/Hz/cell.

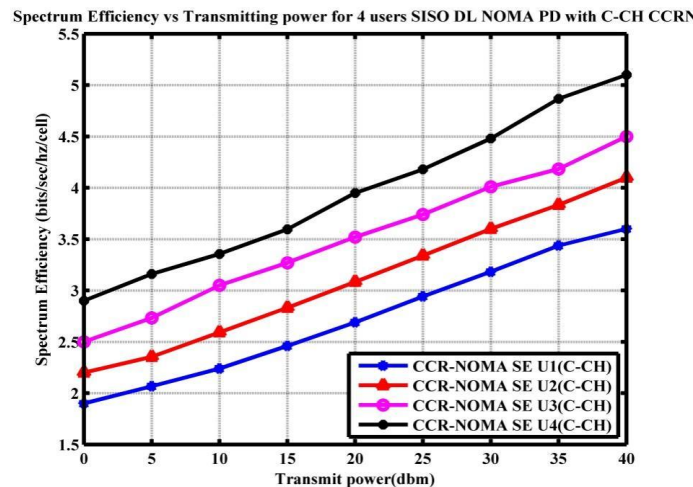


Figure 6. Spectral efficiency for 4 Users Using SISO Downlink NOMA Power Domain with Common Control Channel CCRN

In order to demonstrate the result for the link between spectral efficiency and transmit power with SISO Downlink NOMA with competitive cognitive radio channel. Also, the second model was also simulated a using dedicated channel. In the same scenario where 4 users have varying distances and varying in power coefficients with respect to each other from the base station. Notably, one can observe that maximum spectral efficiency was obtained for the user 4 of about 7.2 bps/Hz/cell having a transmit power setting of about 30dbm (Figure 7).

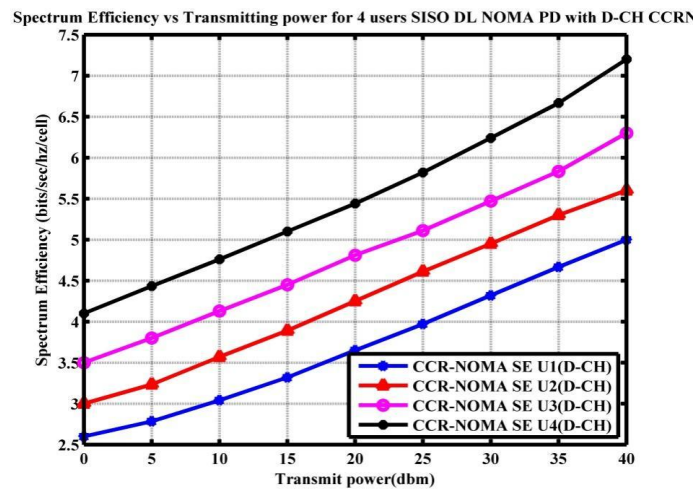


Figure 7. Spectral efficiency vs. Transmitting power for SISO Downlink NOMA Power Domain with Dedicated Channel CCRN

MIMO Downlink NOMA Power Domain

Figure 8 shows the set up for the 64X64 Downlink MIMO NOMA which shows the graphical relationship between 4 users (User 1 to User 4) for varying distances of 800m,600m,300m and 100m from U1 to U4 respectively. These users have different power location coefficients of 0.6,0.3,0.075 and 0.01875 respectively. From the graph, one can observe that the user with the higher power level will have good spectral efficiency. From our scenario, we can see that user 4 which is in close proximity to the base station achieves the highest spectral efficiency as compared with the other 3 users who are comparatively having distance to that of user 4. User 4 archives spectral efficiency of about 12.23 bps/Hz/cell at a rate of 40 dbm transmitting power. User 3 till user 1 then follow the spectral efficiency. With the incorporation of 64X64 MIMO technology still enhances these outcomes further. The performance comparison of user 4 with MIMO and to that of SISO Downlink NOMA there is a significant performance increase in the spectral efficiency can be seen in the case of user 4 with MIMO technique. Approximately about 8.33% increase in the performance of user 4 MIMO to that of user 4 having SISO NOMA. The effectiveness of MIMO technology with NOMA, in terms of improvement in spectral efficiency having unreliable channel conditions can be observed. This performance improvement further leads the way for improvement in the 5g network scenarios to improve communication and also to adapt to various user cases.

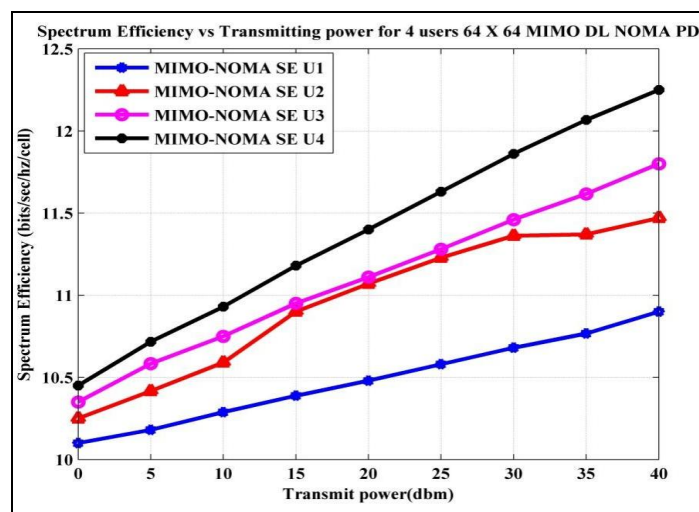


Figure 8. Spectral efficiency vs. Transmitting power for 64 64 MIMO Downlink-NOMA Power Domain.

From Figure 9, one can observe the correlation between the spectral efficiency to that of the power coefficient of 4 user cases situated at a certain distance from the base station having a unique power coefficient. From the

graph, one can analyze that the implementation of 64X64 MIMO Downlink NOMA with coordinated channel resource negotiation for the user 4 have notably high performance in the spectral efficiency by about 17.75 bps/Hz/cell by a transmitting power of 40dbm.

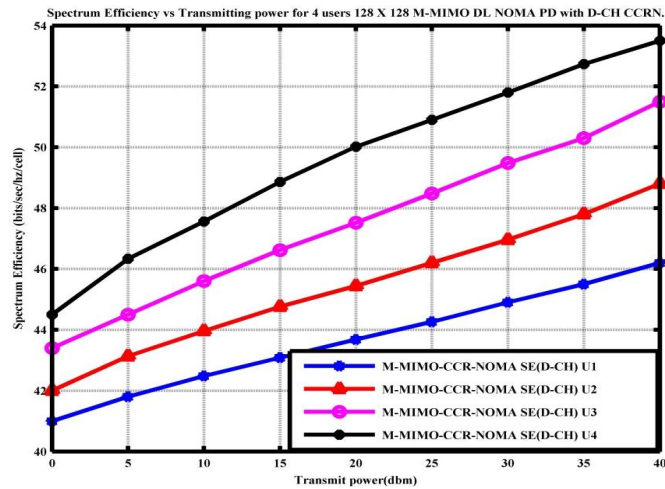


Figure 9. Spectral efficiency against Transmitting Power for 6464 MIMO Downlink NOMA Power Domain with Common Control Channel CCRN

The implementation of 64×64 MIMO technology along with CCRN NOMA for common control channel has significantly improved the performance of spectral efficiency. Among the 4 users, user 4 is the best user which outperforms the SISO Downlink CCR-NOMA power domain for the common control channels by about 12.66 bps/Hz/cell at 40 dBm. This improvement shows how MIMO and CCRN NOMA may optimize spectral efficiency, especially with the common control channel. The results demonstrate the potential benefits of 5G network technology, improving spectral efficiency and communication performance.

Figure 10 below discusses the spectral efficiency for 4 different users having distance variations, and power variations and analyses the performance for 64X64 MIMO Downlink NOMA associated with CCRN and utilizing a dedicated channel. Since the user 4 is so proximity to the base station have the best performance as compared with the other remaining users. The performance has the best spectral efficiency of about 18.81 bps/Hz/cell at a rate of 40dbm.

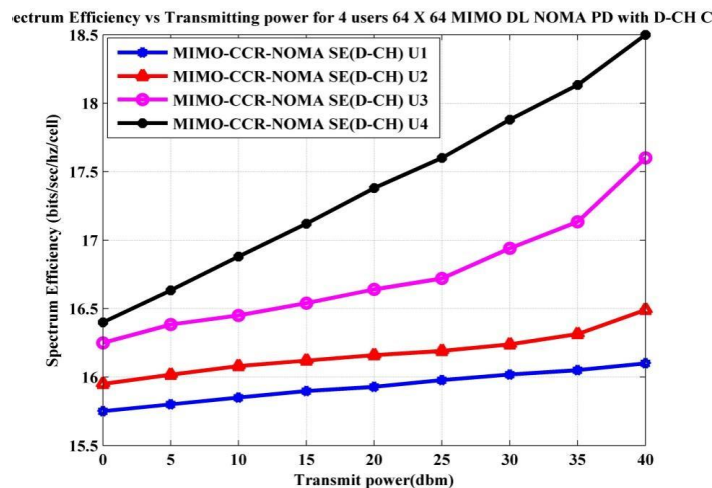


Figure 10. Spectral efficiency vs. Transmitting power for 6464 MIMO Downlink-NOMA Power Domain with Dedicated Channel CCRN

After analyzing the performance of the user 4, having 64X64 MIMO NOMA with CCRN for dedicated channel. There was a significant improvement in the spectral efficiency at transmitting power of 40dbm. When we look into the performance comparison of MIMO to that of SISO Downlink NOMA there was an increase in the performance of about 11.31 bps/Hz/cell. Significantly the performance will surely increase with respect to 5G networks and also by including MIMO technology.

M-MIMO Downlink NOMA Power Domain

Figure 11 depicts the correlation between spectral efficiency and transmit power for four users (U1, U2, U3, and U4) in the 128×128 M-MIMO Downlink NOMA power domain system. The analysis examines various distances and power placement coefficients, demonstrating a continuous trend where higher transmit power is associated with higher spectral efficiency. User U4, located in closest proximity to the base station, demonstrates the most noteworthy spectral efficiency performance, with a rate of 33.89 bps/Hz/cell with a transmit power of 40 dBm. U3, U2, and U1 follow in descending order of the spectral efficiency performance.

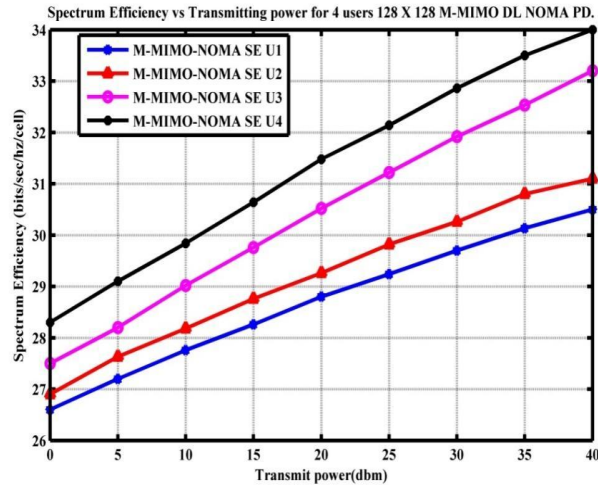


Figure 11. Spectral efficiency vs. Transmitting power for 128 X 128 M-MIMO Downlink NOMA Power Domain

The implementation of 128×128 M-MIMO technology in conjunction with NOMA introduces substantial improvements in spectral efficiency. The most notable enhancement is observed for the best-performing user, U4, who experiences a remarkable increase of 29.99 bps/Hz/cell in spectral efficiency at a transmit power of 40 dBm when compared to the performance of SISO Downlink NOMA power domain. These results highlight the significant impact of advanced M-MIMO technology combined with NOMA schemes in enhancing spectral efficiency within 5G networks (Figure 12).

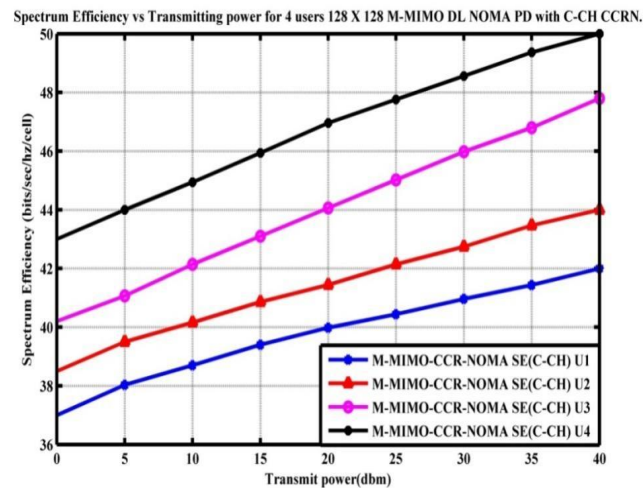


Figure 12. Spectral efficiency against transmitting power for 128×128 M-MIMO Downlink NOMA Power Domain with Common Control CCRN

The findings underscore the potential for achieving superior communication performance, especially in scenarios involving multiple input and output configurations and non-orthogonal multiple access protocols. In Figure 13, the spectral efficiency versus transmit power is depicted for 128×128 Downlink NOMA power domain integration with the CCRN using a common control channel. Notably, at a transmit power of 40 dBm, user U4, in close proximity to the base station, attains the highest spectral efficiency performance at 50.12 bps/Hz/cell.

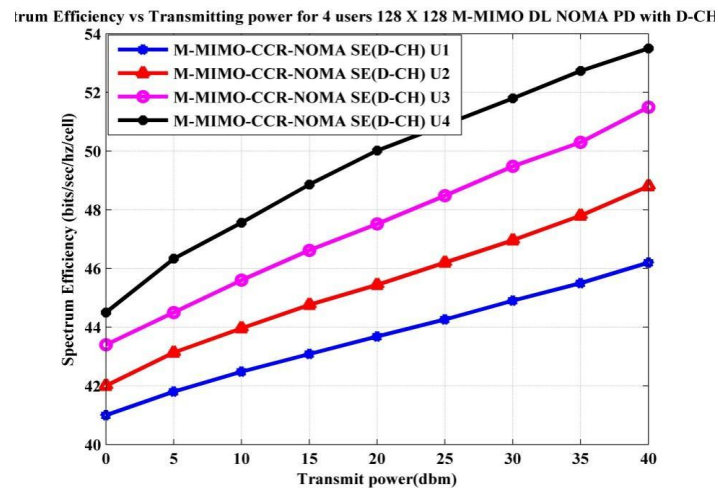


Figure 13. Spectral efficiency vs. Transmitting power for 4 Users' 128 X128 M-MIMO Downlink NOMA Power Domain with Dedicated Channel CCRN

Figure 13 depicts the case for the Massive MIMO NOMA for Downlink which is paired with CCRN with a dedicated channel. Figure 12 above shows the plot of spectral efficiency with that of transmitting power for various users at different locations having varying power coefficients. For the transmission power of 40 dbm, user 4 exhibits the best spectral efficiency at a rate of 52.9 bps/Hz/cell. As compared with this technique with the SISO CCR-NOMA with the dedicated channel, a huge increase in the spectral efficiency by about 46.07 bps/Hz/cell at 40 dbm after incorporating 128X128 MIMO technology.

CONCLUSION

In this research work, the overall effectiveness of the Downlink NOMA power domain for a 5G network is proposed. With respect to spectral efficiency parameters, we have developed a novel method combining SISO, 64X64 MIMO and 128X128 Massive MIMO with a coordinated communication radio network. These methods involve accessing CCRN channels via the competition channel and letting the CCRN meet user channel needs via the dedicated channel. SIC, unstable channels, and Additive white Gaussian noise in Rayleigh fading were considered when placing users at varied distances, programmable logic controllers, and transmission power levels. In a unified network and single cell with coordinated multi-point (CoMP) transmission and reception, 64 64 MIMO and 128 128 M-MIMO technologies improved spectral efficiency. Multiple scenarios showed U4's greater spectral efficiency. At 40 dBm transmit power, they achieved a spectral efficiency of 3.9 bps/Hz/cell with SISO Downlink NOMA, 5.1 bps/Hz with CCRN with the common control channel, and 7.2 bps/Hz with CCRN with the dedicated control Channel. The usage of 64 x 64 MIMO NOMA Downlink significantly improved U4 by 51%. Using 64 x 64 MIMO Downlink NOMA with CCRN (common control channel) and (dedicated control channel) increased spectral efficiency by 64% and 65%, respectively, while preserving transmit power. The adoption of 128 × 128 M-MIMO NOMA improved spectral efficiency by about 79% for U4. Similarly, 128 × 128 M-MIMO Downlink NOMA with CCRN (common control channel) and (dedicated control channel) showed 85% and 86% improvements in spectral efficiency, respectively. The use of SISO 64 × 64 MIMO and 128 × 128 M-MIMO Downlink NOMA systems with CCRN dramatically improved spectral efficiency. The study focuses on expanding users, deploying MIMO technology, using efficient channel coding, massive multiple access methods, and bandwidth shaping to improve spectral efficiency. The exploratory goal is to combine large MIMO cooperative NOMA and cognitive radio for uplinks.

ETHICAL DECLARATION

Conflict of interest: No declaration required. **Financing:** No reporting required. **Peer review:** Double anonymous peer review.

REFERENCES

- [1] L. Dai, B. Wang, Y. Yuan, S. Han, I. Chih-Lin, and Z. Wang, "Non-orthogonal multiple access for 5G: Solutions, challenges, opportunities, and future research trends," *IEEE Communications Magazine*, vol. 53, no. 9, pp. 74-81, 2015.
- [2] S. Timotheou and I. Krikidis, "Fairness for non-orthogonal multiple access in 5G systems," *IEEE Signal Processing Letters*, vol. 22, no. 10, pp. 1647-1651, 2015.
- [3] D. Feng, "Performance comparison on NOMA schemes in high speed scenario," in *2019 IEEE 2nd International Conference on Electronics Technology (ICET)*, May 2019, pp. 112-116.
- [4] M. U. Muzaffar and R. Sharqi, "A review of spectrum sensing in modern cognitive radio networks," *Telecommun Syst* 85, pp. 347-363, 2024, doi: 10.1007/s11235-023-01079-1.
- [5] Z. Chen, Z. Ding, X. Dai, and R. Zhang, "An optimization perspective of the superiority of NOMA compared to conventional OMA," *IEEE Transactions on Signal Processing*, vol. 65, no. 19, pp. 5191-5202, 2017.
- [6] Z. Ding, Z. Zhao, M. Peng, and H. V. Poor, "On the spectral efficiency and security enhancements of NOMA assisted multicast-unicast streaming," *IEEE Transactions on Communications*, vol. 65, no. 7, pp. 3151-3163, 2017.
- [7] M. Hassan, M. Singh, and K. Hamid, "Survey on NOMA and spectrum sharing techniques in 5G," in *2021 IEEE International Conference on Smart Information Systems and Technologies (SIST)*, Apr. 2021, pp. 1-4.
- [8] F. Boccardi et al., "Spectrum pooling in mmWave networks: Opportunities, challenges, and enablers," *IEEE Communications Magazine*, vol. 54, no. 11, pp. 33-39, Nov. 2016, doi: 10.1109/MCOM.2016.1600191CM.
- [9] Y. N. Ahmed, "Analysis of the maximum ratio transmission precoding under imperfect channel state information with hardware impairments in correlated channels," in *2021 IEEE 93rd Vehicular Technology Conference (VTC2021-Spring)*, Helsinki, Finland, 2021, pp. 1-6, doi: 10.1109/VTC2021-Spring51267.2021.9448907.
- [10] M. Dhananjaya, D. Potnuru, P. Manoharan and H. H. Alhelou, "Design and implementation of single-input-multi-output dc-dc converter topology for auxiliary power modules of electric vehicle," *IEEE Access*, vol. 10, pp. 76975-76989, 2022, doi: 10.1109/ACCESS.2022.3192738.
- [11] P. Saritha , V. Devi, A. Babu, and R.P. Praveen, "Design and analysis of multiple input single output converter for hybrid renewable energy system with energy storage capability", *Ain Shams Engineering Journal*, vol. 14, no. 10, p. 102194, Oct. 2023, doi: 10.1016/j.asej.2023.102194.
- [12] G. C. Alexandropoulos, M. A. Islam, and B. Smida, "Full-duplex massive multiple-input, multiple-output architectures: Recent advances, applications, and future directions," *IEEE Vehicular Technology Magazine*, vol. 17, no. 4, pp. 83-91, Dec. 2022, doi: 10.1109/MVT.2022.3211689.
- [13] C. G. Ngobi, M. A. Ahaneku, and O. S. Abayomi, "Channel capacity optimization using multiple-input multiple-output for a rayleigh channel," *European Journal of Electrical Engineering and Computer Science*, vol. 7, no. 6, pp. 96-102, Dec. 2023, doi: 10.24018/ejece.2023.7.6.460.
- [14] Y. Arjoune and N. Kaabouch, "A comprehensive survey on spectrum sensing in cognitive radio networks: Recent advances, new challenges, and future research directions," *Sensors*, vol. 19, no. 1, p. 126, Jan. 2019, doi: 10.3390/s19010126.
- [15] H. B. Salameh, S. Abdel-Razeq and H. Al-Obiedollah, "Integration of cognitive radio technology in NOMA-based b5g networks: State of the art, challenges, and enabling technologies," *IEEE Access*, vol. 11, pp. 12949-12962, 2023, doi: 10.1109/ACCESS.2023.3242645.
- [16] S. Bhattacharjee, T. Acharya, and U. Bhattacharya, "Cognitive radio based spectrum sharing models for multicasting in 5G cellular networks: A survey," *Computer Network*, vol. 208, May 2022.
- [17] A. Nasser, H. A. H. Hassan, J. A. Chaaya, A. Mansour, and K. C. Yao, "Spectrum sensing for cognitive radio: Recent advances and future challenge," *Sensors*, vol. 21, no. 7, p. 2408, Mar. 2021.
- [18] W. S. H. M. W. Ahmad, N. A. M. Radzi, F. Samidi, A. Ismail, F. Abdullah, M. Z. Jamaludin, and M. Zakaria, "5G technology: Towards dynamic spectrum sharing using cognitive radio networks," *IEEE Access*, vol. 8, pp. 14460-14488, 2020.
- [19] Z. M. Bakhsh, J. Z. Moghaddam, and M. Ardebilipour, "An interference management approach for CR-assisted cooperative D2D communication," *AEU-Int. J. Electron. Commun.*, vol. 115, Feb. 2020, doi: 10.1016/j.aeue.2019.153026.
- [20] V. Hassija, V. Chamola, V. Saxena, D. Jain, P. Goyal, and B. Sikdar, "A survey on IoT security: Application areas, security threats, and solution architectures," *IEEE Access*, vol. 7, pp. 82721-82743, 2019.
- [21] H. Shuai, K. Guo, K. An, and S. Zhu, "NOMA-based integrated satellite terrestrial networks with relay selection and imperfect SIC," *IEEE Access*, vol. 9, pp. 111346-111357, 2021.
- [22] L. Lv, J. Chen, Q. Ni, Z. Ding, and H. Jiang, "Cognitive non-orthogonal multiple access with cooperative relaying: A new wireless frontier for 5G spectrum sharing," *IEEE Commun. Mag.*, vol. 56, no. 4, pp. 188-195, Apr. 2018.
- [23] Z. Ali, Y. Rao, W. U. Khan, and G. A. S. Sidhu, "Joint user pairing, channel assignment and power allocation in NOMA based CR systems," *Appl. Sci.*, vol. 9, no. 20, p. 4282, Oct. 2019.
- [24] Z. Ding, R. Schober, and H. V. Poor, "A general MIMO framework for NOMA Downlink and uplink transmission

- based on signal alignment,” *IEEE Trans. Wireless Commun.*, vol. 15, no. 6, pp. 4438–4454, Jun. 2016.
- [25] H. Hu, H. Zhang, H. Yu, Y. Chen, and J. Jafarian, “Energy-efficient design of channel sensing in cognitive radio networks,” *Comput. Electr. Eng.*, vol. 42, pp. 207–220, Feb. 2015.
- [26] A. Nasser, H. A. H. Hassan, J. A. Chaaya, A. Mansour, and K-C. Yao, “Spectrum sensing for cognitive radio: Recent advances and future challenge,” *Sensors*, vol. 21, no. 7, p. 2408, Mar. 2021.
- [27] F. M. Caceres, K. Sithampanathan, and S. Sun, “Theoretical analysis of hybrid SIC success probability under Rayleigh channel for uplink CR-NOMA,” *IEEE Trans. Veh. Technol.*, vol. 71, no. 10, pp. 10584–10599, Oct. 2022.
- [28] D-T. Do, A-T. Le, and B. M. Lee, “NOMA in cooperative underlay cognitive radio networks under imperfect SIC,” *IEEE Access*, vol. 8, pp. 86180–86195, 2020.
- [29] A. Omid, E. Afshin, and M. Nader, “NOMA inspired cooperative relaying system using an AF relay,” *IEEE Wirel. Commun. Lett.*, vol. 8, no. 1, pp. 261–264, 2019.
- [30] G. Im and J. H. Lee, “Outage probability for cooperative NOMA systems with imperfect SIC in cognitive radio networks,” *IEEE Commun. Lett.*, vol. 23, no. 4, pp. 692–695, 2019.
- [31] L. Luo, Q. Li, and J. Cheng, “Performance analysis of overlay cognitive NOMA systems with imperfect successive interference cancellation,” *IEEE Trans. Commun.*, vol. 68, no. 8, pp. 4709–4722, 2020.